

**A NEW TOOL TO INVESTIGATE INFRARED SPECTRA, BASED ON WAVELET FILTERING. APPLICATION TO HAWAII.** A. Gendrin<sup>1</sup> and S. Erard<sup>2</sup>, <sup>1</sup>Institut d'Astrophysique Spatiale, CNRS, Université Paris 11, bâtiment 121, 91405 Orsay Campus, France [aline.gendrin@ias.fr](mailto:aline.gendrin@ias.fr), [erard@ias.fr](mailto:erard@ias.fr).

**Introduction:** A new method to analyze imaging spectrometry data is presented here. The method is based on wavelet filtering of the original data and permits automated detection and characterization of spectral features in large data sets. The method is developed in the frame of the OMEGA/Mars-Express data processing pipe-line. Its capabilities are here assessed on an AVIRIS image cube acquired over the Hawaii volcanoes, where it allows one to identify spectral units consistent with previous, independent studies.

**Method:** The wavelet transform is defined by

$$S(a, b) = \frac{1}{\sqrt{a}} \int g^* \left( \frac{t-b}{a} \right) s(t) dt$$

where  $s(t)$  is the analyzed signal and  $g$  is a 'wavelet'. A wavelet is an oscillating function, with a finite energy and a null mean (e.g. [1]). Examples of two such functions are shown in Fig. 1d and 1f. Conceptually, the wavelet transform consists in comparing the signal with a set of wavelets of different widths, determined by the scale parameter  $a$ . Each wavelet component therefore bears information related to the width (or scale) and location of features present in  $s(t)$ .

The application of the wavelet transform to spectral data is illustrated in Fig. 1. Fig. 1a is a synthetic spectrum obtained by adding the individual Gaussian components presented in Fig. 1b. We used DOG wavelets (Fig. 1d and 1f) as analyzing functions, because their profile is as similar as possible to that of the features to be detected. Fig. 1c and 1e show the two corresponding wavelet components.

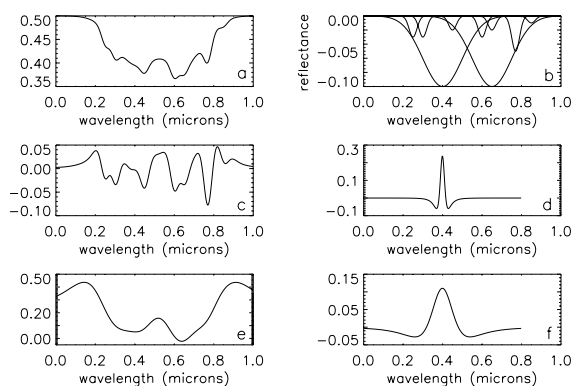


Fig 1: A synthetic spectrum (a) and its wavelet components (c, e)

In this case, bands of various widths are correctly detected even though they overlap strongly. This capacity is potentially very useful in the analysis of near-infrared spectra, where overlapping bands are quite common.

As shown in Fig. 1, each wavelet component presents a minimum at the center of a spectral band, and bands of different widths are detected on different components. The set of scale parameters used is determined so as to minimize redundancy in the decomposition, and to optimize computing time. The main three characteristics of the bands are estimated as described in Fig. 2: The band center is the minimum measured on the wavelet component; the width is the distance between the 2 maxima surrounding this minimum; the depth is estimated from the level of the original spectrum at these three wavelengths.

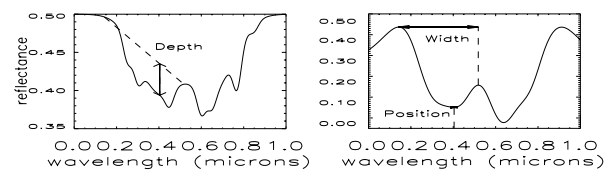


Fig. 2: Illustration of band characteristic estimates. (left) synthetic spectrum from Fig. 1; (right) one of the wavelet components.

Band centers and widths can be detected automatically. The method therefore monitors potential changes in band positions or widths due, for example, to variations in composition, concentrations or grain size between different geological units. The method requires no prior knowledge of the spectra, and no assumption on mineralogical composition or variability. It is therefore well-suited for quick-look analysis of large data sets such as the forthcoming observations from OMEGA on Mars-Express.

The method provides automatic band detection and characterization, and therefore a broad mineralogical composition diagnostic. Its outputs can be used as entry to more quantitative analyzing tools such as fitting algorithms (e.g., MGM [2], [7]), inversion algorithms [3], or classification schemes (e.g. cluster, G-mode).

**Application to AVIRIS observations of Mauna Kea:** The method was tested in particular on an AVIRIS scene of Mauna Kea corrected for atmospheric scattering and extinction, kindly provided by R. Arvidson and E. Guinness. This scene has been extensively studied by [4] and [5], and ground-truth exists for the main geologic units. AVIRIS data have a pixel size of  $\sim 20$  m and a spectral resolution of  $\sim 0.01 \mu\text{m}$ . The original spectra range from 0.4 to  $2.45 \mu\text{m}$ . We studied three spectral subranges separately (like [4]) in order to avoid the remnant atmospheric water absorptions: [0.4-1.3  $\mu\text{m}$ ], [1.5-1.8  $\mu\text{m}$ ], and [2.0-2.5  $\mu\text{m}$ ].

The present method provides a characterization of the various bands present in the spectra, and leads to the identification of regions with homogeneous spectral properties. Mineralogical composition is inferred

from comparison with spectral libraries, and spectral units are delimited using simple groupings. More detailed analyses, or analyses of more complicated data sets, could use specialized algorithms to perform these steps.

Hematite is identified through the presence of the 0.86  $\mu\text{m}$  absorption. Three distinct spectral units appear to be dominated by hematite, with spatial distribution in agreement with [5]. The differences between these three units are likely related to grain size. In regions presenting the deepest 0.86  $\mu\text{m}$  band, two other bands are identified at  $\sim 0.5 \mu\text{m}$  and  $\sim 0.7 \mu\text{m}$ . These 3 bands are easily identifiable on library spectra of coarse-grained hematite. In regions of intermediate 0.86  $\mu\text{m}$  band depth, only the  $\sim 0.5 \mu\text{m}$  band is detected. Finally, only the 0.86  $\mu\text{m}$  is detected wherever this band is the shallowest. This variation is consistent with an increase in grain size. The corresponding units are mapped in Fig. 3.

Three different species of phyllosilicates are identified through the detection of 3 metal-OH bands at slightly different wavelengths in the 2.2-2.3  $\mu\text{m}$  region, again in agreement with [4]. A first band is detected at a wavelength slightly shorter than 2.2  $\mu\text{m}$ . A close examination of the spectra allows the identification of kaolinite. Another band is identified at a wavelength slightly longer than 2.2  $\mu\text{m}$ , indicating montmorillonite. Finally a third band is isolated at a wavelength of  $\sim 2.3 \mu\text{m}$ , indicating saponite. The present method therefore demonstrates its ability to separate very close absorption bands, and to isolate units that present subtle differences in composition.

The base of the cinder cones have spectra with a very narrow spectral absorption at 0.45  $\mu\text{m}$ , characteristic of a steep rise at the beginning of the spectrum, an absorption at 0.6  $\mu\text{m}$ , showing the presence of a slight inflexion at this wavelength, a band at 0.86  $\mu\text{m}$ , signing the presence of a ferric constituent, and 3 other features: a very narrow band at  $\sim 1.13 \mu\text{m}$ , a decrease near 1.3  $\mu\text{m}$  steeper than in other regions, and a steep increase in reflectance near 2  $\mu\text{m}$ , due either to residual atmospheric water absorption or to the presence of an hydrated mineral such as zeolite. These spectral features are consistent with units dominated by palagonitic materials, possibly mixed with an hydrated mineral.

Another absorption located near 0.9  $\mu\text{m}$  is detected on almost every pixel in the scene. The band center is located close to 0.86  $\mu\text{m}$  in regions identified above as hematite-rich. In some areas figured in brown in Fig. 4, this band is located at larger wavelengths ( $\sim 0.9 \mu\text{m}$ ), similar to the band present in spectra of jarosite. On many of the pixels of this unit, the wavelet filter identifies two bands, centered at  $\sim 0.85 \mu\text{m}$  and  $\sim 0.90 \mu\text{m}$ . A very faint absorption is detected for some pixels at  $\sim 2.3 \mu\text{m}$ , as expected for jarosite. [6] showed that an intimate mixture of jarosite with a brighter mineral results in the predominance of jarosite features below 1.4  $\mu\text{m}$ , while the other mineral spectrally dominates

above this wavelength. Therefore, a mixture of palagonite and jarosite could account for the presence of a 0.91  $\mu\text{m}$  band, without (or with a very shallow) absorption at 2.2-2.3  $\mu\text{m}$ , as observed here.

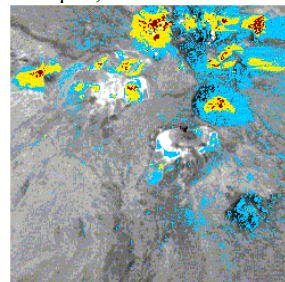


Fig 3: Three hematite units, likely corresponding to a variation in grain size. The brown units contains the finest grain size, the yellow unit the intermediate sizes, and the blue units the coarsest grains.

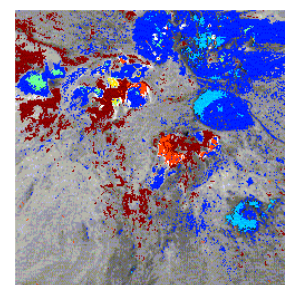


Fig 4: Main spectral units and major materials. Dark blue: hematite; light blue: palagonite; green: montmorillonite; yellow: kaolinite; red: saponite; brown: palagonite/jarosite mixture (tentative).

**Conclusion:** The method presented here allows automatic detection and characterization of absorption bands in large data sets, and is particularly efficient for separating overlapping bands of different widths. The method is well fitted for quick-look analysis of large imaging spectroscopy data sets of areas of unknown composition, such as the forthcoming observations of OMEGA from Mars Express.

The application to the AVIRIS image-cube of Hawaii made possible the quick retrieval of results similar to those of the previous, more detailed studies by [4] and [5]. The analysis is relatively quick, requiring only minutes to hours of CPU on a common desktop computer in the example above (62500 pixels x 256 bands). One limitation is that the method relies on the shape of the spectra, and is therefore sensitive to calibration errors. However, studies of spatially varying signatures can be performed on relative spectra to minimize this effect (see [8] for an application on ISM observations of Phobos).

#### References:

- [1] Mallat (1998), *Academic Press*. [2] Sunshine J.M. et al. (1990) *JGR* 95, 6955-6966. [3] Poulet and Erard, this issue. [4] Guinness E.A. et al. (2001), *LPSC XXXII* Abstract #1659. [5] Guinness E.A. et al. (2001), *AGU Abstract* #P52B-0581. [6] Clark et al. *JGR*, in press. [7] Mustard J.F. et al. (1997), *JGR* 102, 25605-26615. [8] Gendrin and Erard, this issue.